Citation: TANG Ruotian, QIU Hongtong, LU Jian, FENG Chunfang, HAO Mingyang. Influence Factors of Per Capita Delay at Signal-Controlled Intersections [J]. Urban Transport of China, 2023, 21(04): 99−108.

Influence Factors of Per Capita Delay at Signal-Controlled Intersections

TANG Ruotian[1, 2], QIU Hongtong[1], LU Jian[1], FENG Chunfang[1], HAO Mingyang[3]

1. Traffic Management Research Institute of the Ministry of Public Security, Wuxi 214151, Jiangsu, China;
2. Wuxi Huatong Intelligent Transportation Technology Development Co.Ltd., Wuxi 214125, Jiangsu, China;
3. Beijing Key Laboratory of Traffic Engineering, Beijing University of Technology, Beijing 100124, China

Abstract: When optimizing signal-controlled intersections based on per capita delay, researchers often simplify models to estimate per capita delay by using average passenger capacity and average delay per vehicle for different vehicle types. This simplified method ignores certain influential factors of per capita delay. Based on the improved traditional Webster model, this paper presents theoretical proof to demonstrate that per capita delay is significantly influenced by different passenger capacities and arrival sequences of vehicles. An estimation method for per capita delay that combines the improved Webster model with Gaussian mixture model is proposed. The proposed estimation method was tested using VISSIM simulation software under various scenarios, including different traffic volume distributions, arrival sequences of vehicles, proportions of vehicle types, and vehicle passenger capacity distributions. The results show that per capita delay at signal-controlled intersections is affected by the arrival sequence of vehicles with varying passenger capacities and the vehicle type proportions. With these influential factors reflected, the proposed estimation method provides more accurate estimates of per capita delay and the extreme values under non-saturated traffic flow conditions. **DOI:** 10.13813/j.cn11-5141/u.2023.0405-en

Keywords: traffic control; per capita delay; analysis of influence factors; improved Webster model; VISSIM simulation; signal-controlled intersections

0 Introduction

With the development of urban motorization, delay per vehicle (DPV) has long been regarded as a key indicator for signal optimization and control at urban road intersections [1–2]. By introducing a vehicle delay function and considering parameters including queue length, number of stops, signal cycle, and effective green time, intersection signal timing is optimized [3–5]. Vehicle delay can be a primary indicator for evaluating traffic efficiency at signal-controlled intersections [6]. However, considering only the traffic efficiency of motor vehicles is no longer sufficient to meet the demands of urbanization and sustainable transportation development.

The focus of transportation management and research is gradually shifting from vehicles to individuals, incorporating delay per person (DPP) to evaluate passenger experience in response to complex traffic flows with different types of vehicles and the scenario evaluation of various intersection crossing strategies [7–8]. Public buses, which can carry a large number of passengers, are the primary focus of DPP research. Studies have concentrated on optimizing signal timing for buses, setting up bus-only lanes, and developing models to optimize DPP at intersections [9–12]. Some studies have used DPP as a key parameter to reflect the priority of bus passengers, developing signal control optimization models that prioritize buses by allowing more passengers to cross intersections efficiently within a given cycle [13–14]. Studies have also found that considering DPP in signal control optimization models can improve the traffic efficiency of public bus passengers while reducing harmful gas emissions per person [15].

The current research on optimizing traffic based on DPP, such as the optimization of signal-controlled intersections [7, 12, 15], typically estimates DPP by considering the average passenger capacity and DPV of different vehicle types, while ignoring the influence of different vehicle passenger capacities and arrival sequences on DPP. While this does not undermine the effectiveness of using DPP as an optimization objective, it does affect the accuracy of evaluating optimization results. To more accurately reflect DPP experienced by passengers, this study proposes a DPP under adapted Webster model (DPP-AWM) to reveal the impact of different vehicle arrival sequences on DPP at signal-controlled intersections for vehicles with different passenger capacities. Test scenarios are established to verify the application effect of the DPP-AWM under different traffic volumes, vehicle arrival sequences, vehicle type proportions, and vehicle passenger capacity distributions, and to discuss the practical significance of DPP. The exploration of DPP in this study provides a new theoretical foundation for the practical implementation of a people-centered approach to sustainable transportation development, including urban development with a focus on public transport, bus priority design, and the implementation of signal control coordination systems.

Received: 2022-08-08

1 DPP-AWM at signal-controlled intersections

To better illustrate the impact of varying vehicle passenger capacities and arrival sequences on DPP at signal-controlled intersections, this study uses the following example to illustrate the difference between the average based DPP (ADPP) and the distribution based DPP (DDPP) methods. Suppose two vehicles, A and B with different passenger capacities, arrive at an intersection within the same signal cycle. Vehicle A has one passenger while vehicle B has ten passengers. One vehicle arrives during the green light phase and passes through the intersection without delay, while the other vehicle arrives during the red light phase and experiences a delay of one second. The ADPP and DDPP are calculated under different scenarios, as shown in Tab. 1.

Tab. 1 DPP calculation methods at signal-controlled intersections

Calculation method	Scenario	
	Vehicle A carries one passenger without delay, while vehicle B carries 10 passengers with a delay of one second.	Vehicle A carries one passenger with a delay of one second, while vehicle B carries 10 passengers without delay.
ADPP	DPV (s) × average passenger capacity (person·vehicle^{-1}) × total number of vehicles (vehicle)/total number of passengers (person) = 0.5 s	
DDPP	∑ Vehicle delay (s) × corresponding passenger capacity (person)/total number of passengers (person) = 0.910 s	∑ Vehicle delay (s) × corresponding passenger capacity (person)/total number of passengers (person) = 0.091 s

The results indicate that the ADPP method fails to reflect the difference in DPP resulting from the varying arrival sequences of vehicles with different passenger capacities. In contrast, the DDPP method effectively captures the influence of arrival sequences of vehicles with different passenger capacities on the DPP. Consequently, the DPP-AWM method is introduced to estimate DPP more accurately.

1.1 Adapted Webster model

The traditional Webster model relies on the variation in the cumulative arrival and departure of vehicles at intersection inlets, as illustrated by Fig. 1 [16]. Specifically, OA and BA represent the curves of cumulative arrival and departure of vehicles respectively. Assuming no queued vehicles exist at the onset of the red signal phase, the total delay of vehicles throughout one signal cycle is equivalent to the area of triangle OAB in Fig. 1. The DPV at the intersection inlet can be illustrated as follows:

$$DPV=\frac{S_{OAB}}{Cq}=\frac{(C-g)^2}{2C\left(1-q/s\right)}, \tag{1}$$

where S_{OAB} represents the area of triangle *OAB*/(vehicle s); C denotes the signal cycle/s; q represents the vehicle arrival rate/(vehicle s^{-1}); g stands for the green signal phase duration/s; s represents the vehicle departure rate/(vehicle s^{-1}).

If each vehicle carries only one person, DPP is obviously equal to DPV. If there is at least one person in each vehicle, theoretically, the traditional Webster model can still be used to calculate DPP in the same way as calculating DPV. In this case, the passenger capacity of different vehicles can be considered as the point density of triangle *OAB*, and the mass of triangle *OAB* represents the total delay experienced by passengers passing through the intersection. Since the passenger capacity is a random variable independent of signal phase and vehicle arrival quantity, directly solving for the mass of triangle *OAB* can be challenging. Specifically, when the number of people in each vehicle is the same, i.e., the point density of triangle *OAB* is a constant, the traditional Webster model can be used to calculate DPP in the same way as calculating DPV. In this scenario, the calculated DPP is evidently equal to DPV.

To calculate the total delay experienced by passengers in vehicles with different passenger capacities, this study adapts the traditional Webster model to estimate DPP based on the cumulative arrival and departure numbers at intersection inlets, as shown in Fig. 2. OABG represents the curve of cumulative passenger arrivals, while DEFG represents the curve of cumulative passenger departures. When the assumptions of the traditional Webster model remain unchanged, the total delay experienced by passengers within one signal cycle is equal to the shaded area in Fig. 2. DPP at intersection inlets can be calculated as follows:

$$\begin{aligned} DPP&=\frac{S_{OABGH}-S_{DEFGH}}{\sum_{j=1}^{Cq}P_j}\\ &=\frac{1}{\sum_{j=1}^{Cq}P_j}\left(\frac{f}{2q}-\frac{f}{2s}\right)\\ &=\frac{f(s-q)}{2qs\sum_{j=1}^{Cq}P_j}, \end{aligned} \tag{2}$$

where

$$\begin{aligned} f=&\left(0+\sum_{j=1}^{1}P_j\right)+\left(\sum_{j=1}^{1}P_j+\sum_{j=1}^{2}P_j\right)+\cdots\\ &+\left(\sum_{j=1}^{qs(C-g)/(s-q)-1}P_j+\sum_{j=1}^{qs(C-g)/(s-q)}P_j\right). \end{aligned}$$

The following equation can be derived:

$$\begin{aligned} f=&\left[1+\frac{2qs(C-g)}{s-q}\right]\sum_{j=1}^{qs(C-g)/(s-q)}P_j-\\ &2\sum_{j=1}^{qs(C-g)/(s-q)}jP_j, \end{aligned} \tag{3}$$

where S_{OABGH} represents the area of the polygon *OABGH*/(person s); S_{DEFGH} represents the area of the polygon *DEFGH*/(person s); P_j represents the passenger capacity of the j-th arriving vehicle in the current cycle/(person).

To calculate the area of polygon OABGH, the polygon is divided into several trapezoids with the same height, which corresponds to the headway of a vehicle at the time it arrives at the intersection, namely 1/q. Similarly, to calculate the area of polygon DEFGH, the polygon is divided into several trapezoids with the same height, which corresponds to the

headway of a vehicle at the time it leaves the intersection, namely 1/*s*. The terms in each bracket of *f* represent the sum of the upper and lower bases of each trapezoid (the first trapezoid being a triangle), where the upper and lower bases represent the accumulated number of people before and after a vehicle passes through the intersection respectively. It can be seen that, under the condition of relatively fixed traffic volume and signal timing plan at the intersection, the key to estimating DPP lies in estimating the cumulative passenger capacity of arriving vehicles. In equation (3), $\sum_{j=1}^{qs(C-g)/(s-q)} jP_j$ represents the weighted sum of the passenger capacity of vehicles that experience delays within the same signal cycle. The weight *j* represents the order in which vehicles arrive, which implies that the sequencing of vehicle arrivals influences the estimation of DPP. For instance, assuming the number of vehicles arriving at the intersection and the passenger capacity per vehicle remain constant within a signal cycle, DPP reaches its maximum when vehicles with higher passenger capacity arrive first and reaches its minimum when vehicles with lower passenger capacity arrive first, as the signal cycle starts from the red phase in the Webster model. Furthermore, if the arrival sequence of vehicles with similar or equal passenger capacities is altered within the same signal cycle, DPP remains relatively unchanged. However, if the arrival sequence of vehicles with significantly different passenger capacities is modified, DPP will experience a significant change. It is evident that the enhanced Webster model exhibits sensitivity to variations in passenger capacity. Given the substantial proportion of private cars in urban traffic flow, the arrival sequences at intersections for vehicles with high passenger capacity, such as buses and large vehicles, have a more pronounced impact on the DPP.

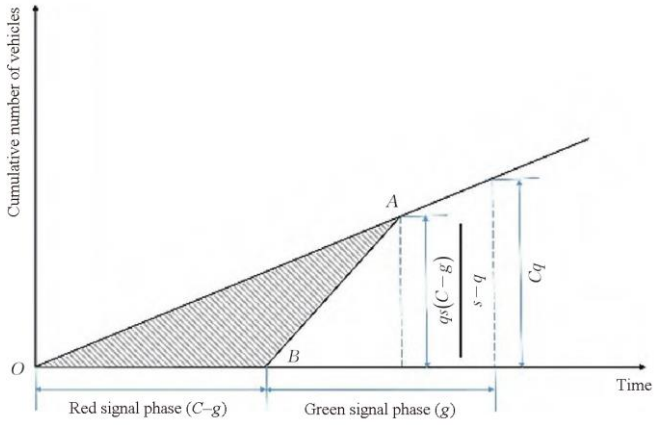

Fig. 1 DPV at signal-controlled intersections

To reflect the impact of average passenger capacity on estimating DPP, the average passenger capacity $\overline{P}$ is used to replace the cumulative sum of vehicle passenger capacity. $\sum_{j=1}^{Cq} P_j = Cq\overline{P}$, $\sum_{j=1}^{qs(C-g)/(s-q)} P_j = \overline{P}qs(C-g)/(s-q)$ and $\sum_{j=1}^{qs(C-g)/(s-q)} jP_j = \overline{P}\sum_{j=1}^{qs(C-g)/(s-q)} j$ are substituted into equations (2) and (3). The result is as follows:

$$DPP = \frac{(s-q)}{2q^2sC\overline{P}}\left\{\left[1+\frac{2qs(C-g)}{s-q}\right]\frac{qs(C-g)}{s-q}\overline{P} - 2\overline{P}\sum_{j=1}^{\frac{qs(C-g)}{s-q}} j\right\} = \frac{(C-g)^2}{2C(1-q/s)}. \quad (4)$$

It can be observed that equation (4) is identical to equation (1), and it is because the underlying assumption of using average passenger capacity is that all vehicles have the same passenger capacity. Therefore, estimating DPP without considering vehicle types using average vehicle capacity essentially becomes an estimation of DPV.

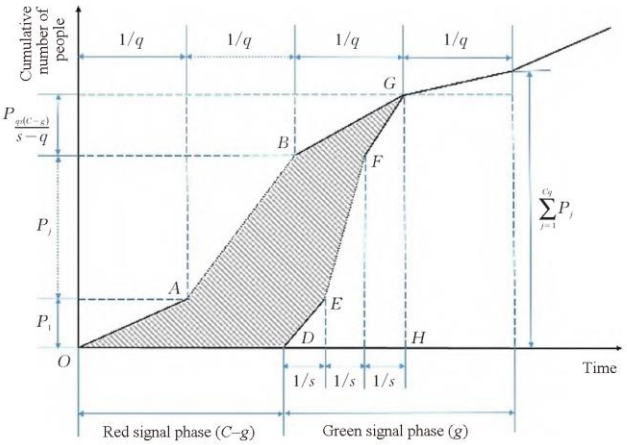

Fig. 2 DPP at signal-controlled intersections

1.2 DPP estimation

It can be inferred from the adapted Webster model that DPP estimation at intersections relies on estimating the passenger capacity of vehicles reaching the intersection and the arrival sequence of vehicles with different passenger capacities. The vehicle passenger capacity is influenced not only by its seating capacity but also by driver or passenger travel behavior and other factors. This study categorizes vehicles affected by the same factors into the same type and assumes that vehicles of the same type follow the same passenger capacity distribution. By collecting information on vehicle capacity in the area where the target intersection is located through resident travel surveys and consultations with public bus operators, the distribution of vehicle capacity can be obtained. Furthermore, the number of vehicle types in the area can be determined based on the number of peaks in the capacity distribution. The DPP-AWM method further assumes that the capacity of vehicles of different types follows different normal distributions and uses a Gaussian mixture model (GMM) to estimate the distribution of vehicle

capacity. The parameters of GMM can be estimated using the expectation-maximization (EM) algorithm.

Although vehicles with different passenger capacities typically arrive at intersections randomly, there is a certain regularity in the order of vehicle arrivals within the same signal cycle due to the intervention of traffic control measures. Therefore, the DPP-AWM method has added the step of optional vehicle sequence adjustment in the adapted Webster model, enabling it to adjust the sequence of vehicle arrivals based on traffic control measures at intersections. For instance, if the intersection implements a strategy that prioritizes the passage of vehicles with high capacities (hereinafter referred to as high-capacity vehicles), such as buses, through early red signal activation or extended green signal duration, these vehicles will pass during the green signal period. By considering pre-existing vehicle queues during the red signal period, high-capacity vehicles will be positioned towards the rear of the traffic flow arriving at the intersection within the same signal cycle. In such cases, the DPP-AWM method estimates DPP by placing high-capacity vehicles at the end of the queue.

The framework of the DPP-AWM method proposed in this study is shown in Fig. 3, and the process of using the DPP-AWM method to estimate DPP within one signal cycle at the target intersection is as follows:

1) The parameter values of GMM are estimated using the EM algorithm based on the passenger capacity data at the target intersection.

2) According to the signal timing and traffic flow data at the target intersection, the number of vehicles experiencing delay a and the number of vehicles passing through the intersection b within one signal cycle are calculated based on the adapted Webster model.

3) b consecutive random sampling is performed using the GMM model to obtain an ordered set of samples $\{P_1, P_2, ..., P_a, ..., P_b\}$, which represent estimated passenger capacities of vehicles arriving at the intersection within one signal cycle. The first a samples correspond to the passenger capacity of delayed vehicles.

4) The sample sequence in $\{P_1, P_2, ..., P_a, ..., P_b\}$ is adjusted according to specific requirements and inputted into the adapted Webster model to estimate DPP.

In practice, it is often necessary to estimate DPP at an intersection over a specific period. For instance, during the dynamic evaluations of signal-controlled intersections, the evaluation time interval is typically set to 2–3 times the signal cycle duration and should not be less than five minutes [17]. The DPP-AWM method can continuously repeat the above estimations and obtain the DPP estimation value over multiple consecutive signal cycles $\sum_{n}^{N}\left(DPP_n\sum_{i}^{b_n}P_{i,n}\right)\Big/\sum_{n}^{N}\sum_{i}^{b_n}P_{i,n}$. DPP_n represents the estimated DPP value in the n-th iteration/s; b_n denotes the number of vehicles passing through the intersection in the n-th iteration/vehicle; $P_{i,n}$ represents the passenger capacity of the i-th vehicle in the n-th iteration/person; N represents the number of consecutive estimations, indicating the number of signal cycles within a specific period. Its value can be adjusted according to practical requirements. In addition to simulating DPP over multiple consecutive signal cycles, the DPP-AWM method also helps mitigate the impact of sampling randomness on the results in GMM by conducting multiple estimations.

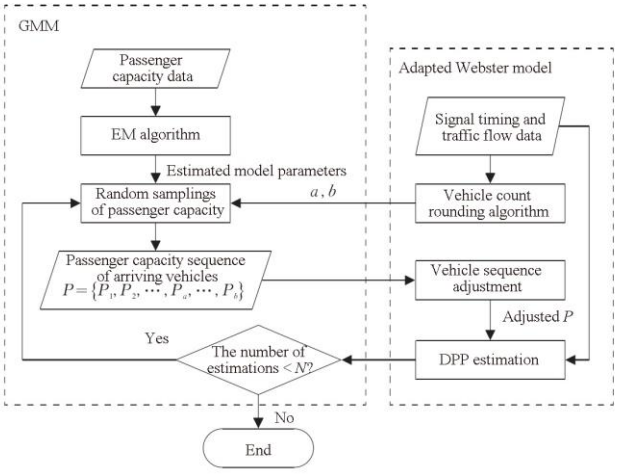

Fig. 3 Framework of DPP-AWM at signal-controlled intersections

Furthermore, due to the fact that in the adapted Webster model, the number of delayed vehicles within one signal cycle qs $(C-g)/(s-q)$ and the number of vehicles passing through the intersection Cq may not be integers, it is necessary to round them to obtain the values of a and b. While simpler methods can be employed to round the vehicle counts, it should be noted that errors can accumulate and amplify with an increasing number of estimations. To mitigate the errors caused by straightforward rounding techniques such as rounding, rounding up, or rounding down, this study proposes a vehicle count rounding algorithm, which follows the steps as follows.

1) The number of delayed vehicles and the number of vehicles passing through the intersection in each estimation are rounded down.

2) The reduced number of delayed vehicles and vehicles passing through the intersection resulting from step 1) is calculated.

3) The computed number of vehicles obtained in step 2) is distributed among the various estimations, and the following two principles should be followed. Firstly, in each estimation, the maximum number of delayed vehicles and vehicles passing through the intersection assigned should not exceed one respectively. Secondly, the number of delayed vehicles in each estimation should always be less than or equal to the number of vehicles passing through the intersection.

2 Experimental design

2.1 Simulation construction

At present, it is difficult to collect the real-time passenger capacity of vehicles at intersections. In this study, the widely used VISSIM simulation software (version 10.0) is employed to create various simulation test scenarios and simulate the passage of vehicles at intersections under different traffic volumes, vehicle arrival sequences, vehicle type proportions, and passenger capacity distributions. The basic settings for intersection channelization, road design, and signal control are kept consistent across different test scenarios.

The focus of the simulations in this study is not to replicate a specific real-world intersection, but to simulate the traffic conditions of multiple possible intersections. Therefore, by referring to the Urban Road Intersection Planning Specification (GB 50647-2011) and the Urban Road Engineering Design Specification (CJJ 37-2012), a signal-controlled intersection is constructed with a cross-shaped configuration where north-south and east-west roads intersect. Each road segment has a length of 150 m with the entrance segment measuring 50 m, consisting of one left-turn lane and one through lane. Vehicles have the freedom to change lanes before entering the entrance segment. The desired speed for each segment is set at 50 km h^{-1}, with a saturation flow rate of 0.533 vehicle s^{-1} for through movements and 0.5 vehicles s^{-1} for left-turn movements. The intersection follows the traditional 4-phase signal control scheme. The total signal cycle length is 100 s, with 25 s for the north-south and east-west through phases and 15 s for the left-turn phases, followed by a 3 s yellow signal phase and a 2 s all-red signal phase between phases. Since right-turning vehicles are not signal-controlled, they are not included in the simulation. According to the durations of the through and left-turn phases, the ratio of through vehicles to left-turn vehicles is set at 5/3. In the simulation, vehicles are categorized as either high-capacity vehicles or low-capacity vehicles, representing medium-sized or larger buses and cars on urban roads respectively. The passenger capacity of vehicles within the same category follows a normal distribution. The total simulation duration for each test scenario is 36 500 s, with vehicle generation based on predetermined traffic volumes, turning proportions, and vehicle type proportions for the first 36 000 s. The vehicle driving behavior and generation method follow the default settings of the simulation software.

2.2 Testing scenarios and parameters setting

In this study, the DPP-AWM method is tested in three different scenarios. In scenario 1, the proportions of vehicle types and passenger capacity distributions are predetermined to simulate the passage of vehicles at intersections under different traffic volumes. In scenario 2, the traffic volume and passenger capacity distributions are predetermined to simulate the passage of vehicles at intersections under different proportions of vehicle types. In scenario 3, the traffic volume and proportions of vehicle types are predetermined to simulate the passage of vehicles at intersections under different passenger capacity distributions.

To reflect the sequence of vehicle arrivals, particularly the impact of the arrival order of high-capacity vehicles, three different vehicle arrival patterns are tested for each scenario. In pattern 1, vehicles of different types arrive randomly, simulating the situation without any optimized traffic control measure. In pattern 2, low-capacity vehicles arrive randomly while high-capacity vehicles arrive during the green signal phase, simulating the scenario where optimized traffic control measures allow high-capacity vehicles to pass through the intersection without stopping, resulting in the minimum DPP. In pattern 3, low-capacity vehicles arrive randomly while high-capacity vehicles arrive at the beginning of the red signal phase, simulating the scenario where the maximum DPP at the intersection is possible. The parameter setting for each scenario is shown in Tab. 2.

Tab. 2 Scenario parameters setting

Scenario	Traffic volume on road segments/ (vehicle·h^{-1})	Proportion of high-capacity vehicles/%	Passenger capacity distributions for high-capacity vehicles (mean, standard deviation)	Passenger capacity distributions for low-capacity vehicles (mean, standard deviation)	Number of simulation runs
Scenario 1	300–700	10	(40, 10)	(2, 0.8)	15
Scenario 2	300	10–90	(40, 10)	(2, 0.8)	27
Scenario 3	300	50	(30–70, 10)	(2, 0.8)	15

1) Traffic volume on road segments

According to the simulation settings, the theoretical saturated flow rate = 3 600/100 ×25 × 0.533 + 3 600/100 × 15 × 0.5 = 749.7 vehicle h^{-1}. It is observed from the actual simulation results that when the traffic volume exceeds 600 vehicles h^{-1} in all directions of the intersection, the traffic flow will reach a saturated state. To ensure a certain delay at the intersection, the minimum traffic volume for each road segment is set to 300 vehicles h^{-1}. Therefore, the traffic volume range for scenario 1 is set to 300–700 vehicles h^{-1}. As one of the assumptions of the Webster model is non-saturated traffic flow, the traffic volume for each road segment in scenarios 2 and 3 is set to 300 vehicles h^{-1}.

2) Proportion of high-capacity vehicles

To ensure that both types of vehicles occupy a certain proportion on the road segment, the proportion of high-capacity vehicles in scenario 2 is set to vary between 10% and 90%. Since high-capacity vehicles account for a smaller proportion in actual road traffic flow, the proportion of high-capacity vehicles in scenario 1 is set to 10%. To eliminate the sensitivity differences in the model under different passenger capacity distributions caused by an imbalance in vehicle types, the proportion of high-capacity vehicles in scenario 3 is set to 50%.

3) Passenger capacity distribution

In comparison to high-capacity vehicles, the variation in passenger capacity of low-capacity vehicles has a negligible impact on DPP. Since the passenger capacity of cars on urban roads is generally 1–5 people, the mean of the passenger capacity distribution for low-capacity vehicles in all scenarios is set to two, and the standard deviation is set to 0.8. High-capacity vehicles are typically public transport vehicles, and their seating capacity determines the mean of the passenger capacity distribution, while passenger demand determines the standard deviation. To simplify the simulation process, this study does not account for variations in passenger demand. Therefore, the standard deviation of the passenger capacity distribution for high-capacity vehicles in all scenarios is set to 10. Under the specifications in Type Classification and Grading Evaluation of Buses (JT/T 888–2020) and Calculation Method for Passenger Vehicle Load Quality (GB/T 12428–2005), the mean of the passenger capacity distribution for high-capacity vehicles in scenario 3 is set to vary between 30 and 70 people, while in scenarios 1 and 2, the mean value is fixed to 40 people.

2.3 Evaluation method

In this study, the signal timings and saturation flow rates for the same turning movements are consistent across different road segments. Therefore, DPP for the same turning movement is calculated by aggregating the results from each road segment. Since the simulation software can output the delay and passenger load of each vehicle directly, the DPP can be calculated directly from the simulation results. To estimate DPP under different scenarios and vehicle arrival patterns using the DPP-AWM method, the number of consecutive estimations is set to 100. Due to the significant differences in DPP, this study uses the absolute percentage error (APE) to evaluate the accuracy of the estimated DPP under different scenarios and vehicle arrival patterns, which can be expressed as follows:

$$APE = \frac{|DPP_T - DPP|}{DPP_T} \times 100\% ,$$

where DPP_T represents the simulated DPP to be estimated/s; DPP represents the estimated DPP/s.

To objectively evaluate the accuracy of the DPP-AWM method, it is compared with the commonly used average based DPP model (ADPP-M). The estimated DPP using the ADPP-M method is calculated as $\sum_{k=1}^{K} \overline{d}_k q_k \overline{P}_k \Big/ \sum_{k=1}^{K} q_k \overline{P}_k$. $\overline{d}_k$ represents the DPV for the k-th category of vehicles/s; q_k represents the flow rate of the k-th category of vehicles/(vehicle s^{-1}); $\overline{P}_k$ represents the average passenger capacity for the k-th category of vehicles/person.

3 Results and analyses

3.1 Scenario 1: DPP estimation under different traffic volumes

In scenario 1, a total of 15 simulations under five different traffic volume conditions are conducted for each of the three vehicle arrival patterns. The results for DPP and DPV are shown in Fig. 4.

Since the vehicle arrival patterns have no impact on the number of vehicles generated in the simulation, DPV remains the same for different arrival patterns. However, DPP increases with an increase in traffic volume for all vehicle arrival patterns. Under the same traffic volume conditions, DPP in pattern 1 is approximately equal to the average of patterns 2 and 3 as well as DPV. This suggests that while the sequence of vehicle arrivals does impact DPP, this influence diminishes when vehicles arrive randomly at intersections over a sufficiently long observation period.

The average APE and the APE differences under different patterns for the DPP-AWM method and ADPP-M method in scenario 1 are shown in Tab. 3. The results are as follows.

1) When the traffic volume of the road segment changes, the DPP-AWM method, compared to the commonly used ADPP-M method, achieves an average improvement of 31.1% in the accuracy of DPP estimation for through vehicles and an average improvement of 17.3% in the accuracy of DPP estimation for left-turn vehicles.

2) Compared to pattern 1, the DPP-AWM method exhibits a greater improvement in the accuracy of DPP estimation in patterns 2 and 3. This indicates that the DPP-AWM method effectively captures the influence of different arrival sequences of vehicles with varying passenger capacities on DPP estimation.

3) Due to the limitation of the traditional Webster model's assumption of non-saturated traffic flow, although the DPP-AWM method can provide more accurate DPP estimation under non-saturated traffic conditions, its estimation accuracy is generally lower when the traffic flow reaches saturation.

3.2 Scenario 2: DPP estimation for different vehicle type ratios

In scenario 2, a total of 27 simulations are conducted for the three vehicle arrival patterns under nine different ratios of high-capacity vehicles. The results for DPP and DPV are shown in Fig. 5.

Similar to scenario 1, under the same ratio of high-capacity vehicles, DPP in pattern 1 is approximately equal to the average values in patterns 2 and 3 as well as DPV. The variation of DPP in pattern 1 is relatively stable, indicating that when vehicles arrive randomly, DPP is less affected by the ratio of vehicle types. The increased ratio of high-capacity vehicles indicates the decreased difference in DPP between pattern 2 and pattern 3, implying a reduced impact of vehicle arrival sequence on DPP.

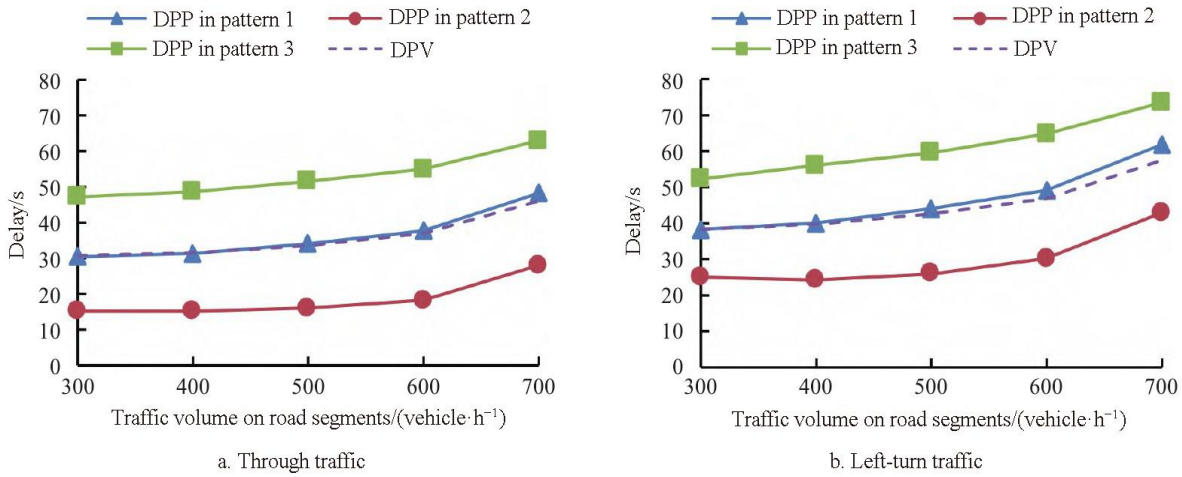

Fig. 4 DPP and DPV in scenario 1

Tab. 3 Comparison of DPP estimation accuracy in scenario 1

Through traffic volume/(vehicle·h^{-1})	Pattern 1		Pattern 2		Pattern 3		Left-turn traffic volume/(vehicle·h^{-1})	Pattern 1		Pattern 2		Pattern 3	
	DPP-AWM method	ADPP-M method	DPP-AWM method	ADPP-M method	DPP-AWM method	ADPP-M method		DPP-AWM method	ADPP-M method	DPP-AWM method	ADPP-M method	DPP-AWM method	ADPP-M method
300	1.6	3.8	33.1	91.8	10.5	38.1	300	0.2	3.3	11.1	48.1	7.7	29.3
400	4.3	5.6	24.7	95.5	5.7	39.1	400	0.8	6.7	10.0	53.7	7.7	33.6
500	1.5	12.2	16.5	86.9	5.8	41.9	500	9.8	14.7	2.4	44.8	7.6	36.9
600	6.5	19.5	6.0	66.4	4.0	44.8	600	17.0	22.8	17.5	25.3	11.6	41.6
700	26.3	36.0	36.1	30.2	13.3	51.0	700	32.7	38.3	44.3	11.0	18.3	48.1
Average *APE*	8.0	15.4	23.3	74.2	7.9	43.0	Average *APE*	12.1	17.2	17.1	36.6	10.6	37.9
APE differences [1)]	7.4		50.9		35.1		*APE* differences [1)]	5.1		19.5		27.3	

1) The average *APE* of the ADPP-M method minus the average *APE* of the DPP-AWM method.

The average *APE* and the *APE* differences under different patterns for the DPP-AWM method and ADPP-M method in scenario 2 are shown in Tab. 4. The results are as follows.

1) When the ratio of vehicle types changes, the DPP-AWM method, compared to the commonly used ADPP-M method, achieves an average improvement of 29.2% in the accuracy of DPP estimation for through vehicles and an average improvement of 14.6% in the accuracy of DPP estimation for left-turn vehicles.

2) Scenario 2 also demonstrates that the DPP-AWM method can effectively reflect the impact of different arrival sequences of vehicles with different passenger capacities on DPP estimation.

3) As the proportion of high-capacity vehicles increases, the estimation accuracy of the ADPP-M method gradually becomes closer to that of the DPP-AWM method. This suggests that an increase in the proportion of high-capacity vehicles reduces the impact of vehicle arrival sequence on DPP estimation, leading to a decrease in the DPP variability across different signal cycles.

3.3 Scenario 3: DPP estimation for different passenger capacity distributions

In scenario 3, a total of 15 simulations are conducted for the three vehicle arrival patterns under five passenger capacity distributions of high-capacity vehicles. The only change made was the passenger volume distribution, specifically altering the average passenger volume. The results for DPP and DPV are shown in Fig. 6.

Similar to scenarios 1 and 2, under the same average passenger capacity conditions of high-capacity vehicles, DPP in pattern 1 is approximately equal to the average values in patterns 2 and 3 as well as DPV. In scenario 3, DPP in all patterns does not vary with changes in the average passenger capacity, indicating that the average passenger capacity has no impact on DPP.

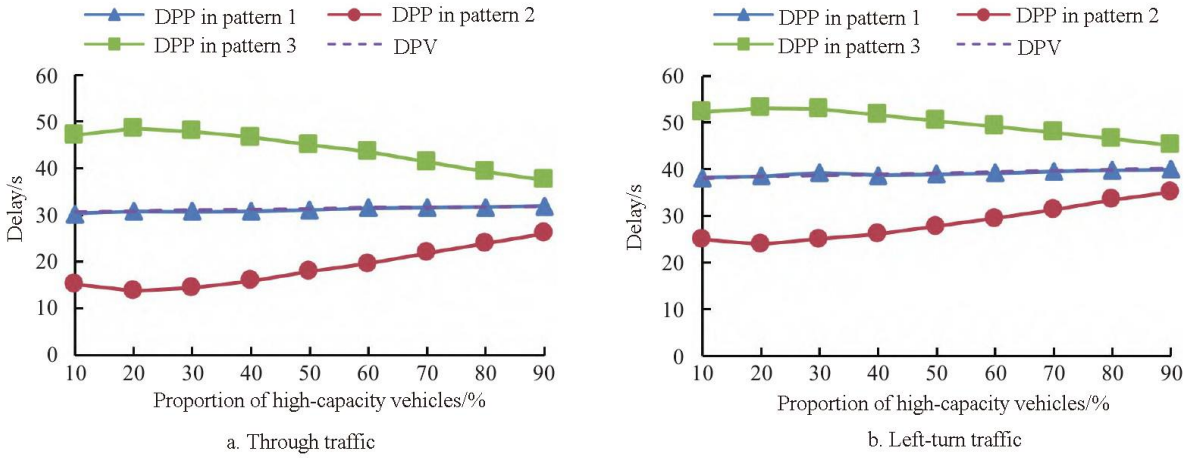

Fig. 5 DPP and DPV in scenario 2

Tab. 4 Comparison of DPP estimation accuracy in scenario 2

Proportion of through high-capacity vehicles/%	Pattern 1		Pattern 2		Pattern 3	
	DPP-AWM method	ADPP-M method	DPP-AWM method	ADPP-M method	DPP-AWM method	ADPP-M method
10	1.6	3.8	33.1	91.8	10.5	38.1
20	0.6	6.1	22.0	109.4	6.6	40.3
30	0.2	5.4	8.3	101.2	2.8	39.2
40	0.2	5.0	3.7	84.0	0.4	37.2
50	0.5	4.7	5.2	65.2	0.6	34.3
60	1.9	5.2	5.4	51.5	1.8	31.4
70	2.1	4.5	4.7	37.6	0	27.1
80	2.5	3.8	4.9	27.3	0.8	22.5
90	3.1	3.5	3.4	18.4	1.8	17.8
Average *APE*	1.4	4.7	10.1	65.2	2.8	32.0
APE differences [1)]	3.3		55.1		29.2	

Proportion of left-turn high-capacity vehicles/%	Pattern 1		Pattern 2		Pattern 3	
	DPP-AWM method	ADPP-M method	DPP-AWM method	ADPP-M method	DPP-AWM method	ADPP-M method
10	0.2	3.3	11.1	48.1	7.7	29.3
20	1.5	4.5	5.2	53.7	3.9	30.7
30	3.4	5.9	6.1	46.7	0.6	30.3
40	2.0	4.3	12.1	41.9	2.6	28.2
50	4.3	4.0	16.2	34.3	4.3	25.9
60	3.7	4.2	15.6	27.0	4.3	23.8
70	2.0	4.5	14.4	20.4	4.3	21.2
80	3.8	4.6	14.4	13.6	2.0	18.3
90	4.6	4.2	10.8	8.9	1.3	15.3
Average *APE*	2.8	4.4	11.8	32.7	3.4	24.8
APE differences [1)]	1.6		20.9		21.4	

The average APE and the APE differences under different patterns for the DPP-AWM method and ADPP-M method in scenario 3 are shown in Tab. 5. The results are as follows.

1) When the average passenger capacity of high-capacity vehicles changes, the DPP-AWM method, compared to the commonly used ADPP-M method, achieves an average improvement of 32.0% in the accuracy of DPP estimation for through vehicles and an average improvement of 13.9% in the accuracy of DPP estimation for left-turn vehicles.

2) Scenario 3 further confirms that the DPP-AWM method can effectively reflect the impact of different arrival sequences of vehicles with different passenger capacities on DPP estimation.

4 Conclusions and prospects

In the existing research on signal-controlled intersection optimization based on DPP, DPP estimation using the average passenger capacity of different vehicle types and DPV fails to consider the impact of the arrival sequences of vehicles with varying passenger capacities on DPP. Therefore, this study proposes the DPP-AWM method by combining the adapted Webster model and GMM. DPP experienced by passengers in various turning movements at intersections is simulated using the simulation software under different traffic volumes, vehicle arrival sequences, vehicle type proportions, and vehicle passenger capacity distributions. Furthermore, a comparative analysis between the DPP-AWM method and the commonly used ADPP-M method is performed. The conclusions are as follows.

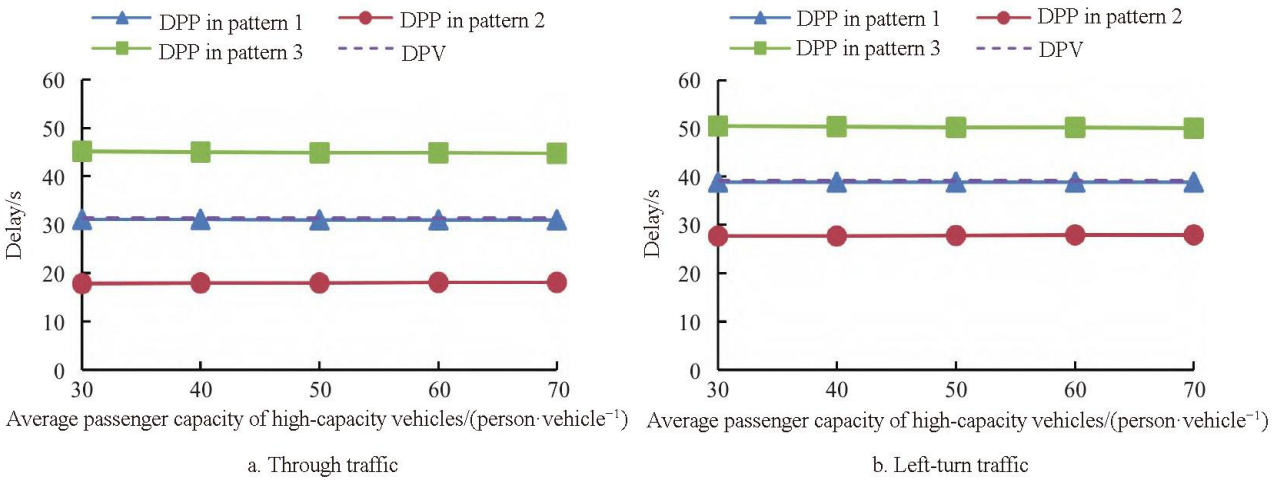

Fig. 6 DPP and DPV in scenario 3

Tab. 5 Comparison of DPP estimation accuracy in scenario 3

Average passenger capacity of through high-capacity vehicles/person	Pattern 1		Pattern 2		Pattern 3	
	DPP-AWM method	ADPP-M method	DPP-AWM method	ADPP-M method	DPP-AWM method	ADPP-M method
30	0.2	4.8	4.8	66.4	0.1	34.5
40	2.1	4.7	6.9	65.2	1.3	34.3
50	0.8	4.7	6.1	64.4	0.1	34.1
60	1.4	4.6	5.9	63.9	0.6	34.1
70	1.1	4.6	5.7	63.5	0.2	34.0
Average *APE*	1.1	4.7	5.9	64.7	0.5	34.2
APE differences [1)]	3.6		58.8		33.7	

Average passenger capacity of left-turn high-capacity vehicles/person	Pattern 1		Pattern 2		Pattern 3	
	DPP-AWM method	ADPP-M method	DPP-AWM method	ADPP-M method	DPP-AWM method	ADPP-M method
30	1.5	4.0	14.5	34.9	3.6	26.2
40	3.8	4.0	16.2	34.3	3.8	25.9
50	2.1	4.0	15.7	33.9	5.8	25.7
60	1.5	4.0	15.9	33.6	6.1	25.6
70	0.7	4.1	14.9	33.4	5.1	25.5
Average *APE*	1.9	4.0	15.4	34.0	4.9	25.8
APE differences [1)]	2.1		18.6		20.9	

1) Although DPP at signal-controlled intersections is affected by the arrival sequences of vehicles with different passenger capacities, the impact diminishes and eventually dissipates as the observation time increases when vehicles arrive at the intersection randomly. With a sufficiently long observation time, DPP experienced by passengers in randomly arriving vehicles becomes equivalent to DPV.

2) The mean passenger capacity distribution among different vehicle types does not exert an impact on DPP, implying that the seating capacity of vehicles does not affect DPP. However, the proportions of different vehicle types do affect DPP. Specifically, the proportion of high-capacity vehicles determines the extreme value of DPP at intersections. Additionally, the increased proportion of high-capacity vehicles indicates the diminished influence of vehicle arrival sequences on DPP.

3) In comparison to the commonly used ADPP-M method, the proposed DPP-AWM method in this study effectively captures the impact of vehicle arrival sequences on DPP and provides more accurate estimations of DPP and its extreme values at different turns of intersections under non-saturated traffic flow conditions. It enhances the comprehensive evaluative capacity of DPP at signal-controlled intersections.

Further improvements can be made in this study. 1) The precision of DPP estimation can be improved using the DPP-AWM method under saturated or oversaturated traffic flow conditions. 2) A more exact vehicle arrival sequence prediction model can be established to replace the step of vehicle sequence adjustment in the DPP-AWM method. 3) Real-world data on vehicle passenger capacities and vehicle delay at intersections can be used to test the DPP-AWM method.

References

[1] QADRI S S S M, GÖKÇE M A, ONER E. Stateof-art review of traffic signal control methods: challenges and opportunities [J]. European transport research review, 2020, 12(1): 1−23.

[2] D'ANS G C, GAZIS D C. Optimal control of oversaturated store-and-forward transportation networks [J]. Transportation science, 1976, 10(1): 1−19.

[3] TALMOR I, MAHALEL D. Signal design for an isolated intersection during congestion [J]. Journal of the operational research society, 2007, 58(4): 454−466.

[4] SCHMÖECKER J D, AHUJA S, Bell M G H. Multi-objective signal control of urban junctions-framework and a London case study [J]. Transportation research part C: emerging technologies, 2008, 16(4): 454−470.

[5] RIBEIRO I M, SIMÕES M L O. The fully actuated traffic control problem solved by global optimization and complementarity [J]. Engineering optimization, 2016, 48(2): 199−212.

[6] JIA R, DAI S H, HUANG N, et al. Literature review on traffic congestion identification methods [J]. Journal of South China University of Technology (nature science edition), 2021, 49(4): 124−139. (in Chinese)

[7] LI J, JIA T Y. Signal timing optimization for intersection based on per capita delay [J]. Journal of highway and transportation research and development, 2021, 38(11): 134−141. (in Chinese)

[8] FENG T J, SUN X L, HUANG J S, et al. Twophase signal intersection delay based on three street crossing modes [J]. Journal of Jilin University (engineering and technology edition), 2022, 52(3): 550−556. (in Chinese)

[9] QIAO W X, WANG D. A transit signal priority optimizing model based on reliability [J]. Journal of transportation systems engineering and information technology, 2017, 17(2): 54−59. (in Chinese)

[10] WANG Y R, LIU Y G, ZHENG S. Transit priority control based on presignal and contraflow left-turn lane [J]. Journal of transportation systems engineering and information technology, 2022, 20(3): 68−80. (in Chinese)

[11] LI S, HAO W. Research on the model of the per capita delay of signal control intersection with bus lane [J]. Highway engineering, 2017, 42(3): 37−39. (in Chinese)

[12] XU J J, FENG P F. Bus-specific import lane setting strategy for intersections based on per capita delay [J]. Journal of Anshun University, 2019, 21(1): 124−127. (in Chinese)

[13] CHANG Y T. Passenger delay based optimal timing model for a signal intersection [J]. Journal of Hunan University (natural sciences), 2009, 36(9): 22−26. (in Chinese)

[14] JIAO P P, LI Z H, LIU M Q, et al. Real-time traffic signal optimization model based on average delay time per person [J]. Advances in mechanical engineering, 2015, 7(10): 1−11.

[15] LIU C, WEI L Y. Signal timing optimization model considering per capita delay and per capita emissions [J]. Journal of Harbin Institute of Technology, 2018, 50(9): 83−88. (in Chinese)

[16] WEBSTER F V. Traffic signal settings [R]. London: Road Research Laboratory, 1958.

[17] The Ministry of Public Security of the PRC. Evaluation methods for road traffic congestion levels: GA/T 115—2020 [S]. Beijing: Standards Press of China, 2020. (in Chinese)

